On the possibilities of hard X-ray imaging with high spatio-temporal resolution using polychromatic synchrotron radiation

A. Rack

*European Synchrotron Radiation Facility, Grenoble, France**

F. García-Moreno

Helmholtz Zentrum Berlin für Materialien und Energie, Institute of Applied Materials, Germany

C. Schmitt and O. Betz

Zoologisches Institut, Abteilung Evolutionsbiologie der Invertebraten, Universität Tübingen, Germany

A. Cecilia and A. Ershov

Institute for Synchrotron Radiation – ANKA, Karlsruher Institut für Technologie, Germany

T. Rack

Charité – Dept. of Maxillofacial and Facial-Plastic Surgery, Division of Oral Medicine, Radiology and Surgery, Berlin, Germany

J. Banhart and S. Zabler

Technical University of Berlin, Institute for Materials Science and Technology, Germany

(Dated: July 20, 2010)

Abstract

Time-resolved imaging with penetrating radiation has an outstanding scientific value but its realisation requires a high density of photons as well as corresponding fast X-ray image detection schemes. Bending magnets and insertion devices of third generation synchrotron light sources offer a polychromatic photon flux density which is high enough to perform hard X-ray imaging with a spatio-temporal resolution up to the µm-µs range. Existing indirect X-ray image detectors commonly used at synchrotron light sources can be adapted for fast image acquisition by employing CMOS-based digital high speed cameras already available on the market. Selected applications from life sciences and materials research underline the high potential of this high-speed hard X-ray microimaging approach.

Keywords: Synchrotron radiation, X-ray imaging, radioscopy, CMOS, cineradiography, microtomography, scintillator, X-ray phase contrast, X-ray detector, real time experiment, digital radiography

*Corresponding author's address: A. Rack, ESRF, BP 220, 38043 Grenoble Cedex, France, tel: +33 (0)476 88 1781, fax: +33 (0)476 88 2785, e-mail: arack@snafu.de

I. INTRODUCTION

The insights provided by moving images can be deep but capturing such images is challenging. The outstanding scientific value of even early motion pictures is demonstrated by the famous movies showing the collapse of the Tacoma Narrows Bridge (USA) in 1943 [1]. An analysis of this problem of non-linear dynamics would not be possible if only a few individual photographic images were available [2]. In order to study events which take place on a time scale shorter than the common video frame rate, high image acquisition speed is required: already at the beginning of the past century, scientists like Lucien Bull developed techniques for high-speed visible-light imaging to study, e. g., the biomechanics of living insects [3]. To achieve comparable imaging frame rates with penetrating radiation is challenging, mainly due to the limited available photon flux density. In special cases, such as periodic movements, one can overcome this issue, for example by choosing a stroboscopic approach (cf., e. g., Kardjilov et al. [4]).

Several so-called third-generation synchrotron light sources have been in operation now for many years all over the world. The polychromatic hard X-ray radiation provided by either bending magnets or insertion devices is intense enough to image aperiodic movements continuously with high time resolution. With the ongoing detector development, microradiography can be developed further towards microradioscopy, allowing one to visualize internal structures of opaque objects as they change with time. The ultimate limit of reachable time resolution is defined by the detector electronics as well as the bunch structure of the electron current inside the synchrotron's storage ring. For the latter case, single-shot imaging using isolated bunches has been reported [5].

A further advantage of using a synchrotron light source is the partial coherence of the emitted wavefronts at the position of the experiment. This allows one to use interference effects as a contrast mode, called 'inline X-ray phase contrast' [6, 7, 8]. This method is much more sensitive than plain attenuation contrast and therefore relaxes the demands on the photon flux density. For a further introduction into the techniques of synchrotron-based microimaging the reader is referred to the literature [9, 10].

In this article, we introduce the basics of the instrumentation needed to perform synchrotron-based imaging with a high spatio-temporal resolution up to the µm-µs range. One of the important aspects is that common indirect detectors available can be modified with minor development effort, by using high speed cameras already available on the market.

Equally important is that with simple bending magnet beamlines, i. e. with a moderate photon flux density, cutting edge investigations can be performed. Several selected applications from life sciences and materials research, employing frame rates from a few hundred up to several 10 000 images/s, underline the high potential of this approach and aim at stimulating further developments at other light sources. The possibility of an extension towards time-resolved three-dimensional imaging (i. e., microtomography) is shown.

II. INDIRECT X-RAY IMAGE DETECTORS

The development of high resolution X-ray imaging detectors for *in situ* investigations with a given time resolution dates back to the late 1960s: so-called live topography was developed to study online the growth of crystals [11]. At that time, an approach based on modified television cameras was employed where X-ray photons are directly converted into electrons that are then registered. Presently, this scheme is commonly called 'direct detection' and has been further developed using more sophisticated (electronic) concepts. In the middle of the 1970s, first detectors were reported in combination with live topography that use a scintillator screen to convert X-rays into visible light (similar to the medical technique *fluoroscopy*). The resulting luminescence image is projected via diffraction-limited visible light optics onto a camera [12]. This frequently called 'indirect detection' scheme was applied in the early 1980s in combination with synchrotron radiation sources, again to perform live topography [13]. Indirect detectors have the advantage of providing high resolutions as well as containing mostly components that are commercially available. The reachable spatial resolution is determined by the scintillating screen and the numerical aperture of the objective used (restricted by Abbe's theorem) [14, 15]. Further concepts for high resolution X-ray imaging detectors were developed for astronomical measurements [25].

Also during the 1980s, the development of synchrotron-based X-ray imaging started. It promised to reach a high performance in terms of both spatial resolution and contrast due to the available high photon flux density compared to laboratory based sources as well as the nearly parallel propagation of synchrotron light [16]. One of the aims to be reached was to transfer the already pioneered microtomography techniques to the synchrotron storage rings [9, 17, 18, 19, 20, 21, 22]. The most promising approach to reach high spatial resolutions was the combination of the indirect detection scheme with CCD cameras [23, 24].

In the 1990s, a design was established that basically uses a visible-light microscope with a folded beam path to project luminescence images from the scintillator onto the CCD camera – optimised for spatial resolution, while partially compromising on the efficiency and the field of view [26] – cf. Fig. 1 (left). Such detectors can reach a resolving power in the (sub-)micrometre range as standard application when transparent single-crystal thin film scintillators are employed [15]. For high photon flux densities in combination with a harder spectrum and corresponding heat loads, the visible light optics directly behind the scintillator can be damaged and/or deteriorate the resolution, e. g., in case they start to emit fluorescent X-rays. In order to avoid this, a long working distance objective is used instead of the visible light microscope. It projects the image through the mirror onto the camera [27, 28] – cf. Fig. 1 (right). The latter approach is also used in neutron imaging [4, 29]. For moderate photon energies, so-called inline versions of the optics shown can be employed [30].

The original application of indirect detectors, live topography (using polychromatic hard X-ray synchrotron radiation) as well as *ex situ* topography is of course benefitting from these developments as well [31, 32]. Further review articles on high-resolution detectors for synchrotron-based hard X-ray imaging, CCD-based X-ray detection schemes as well as direct pixel area detectors have been published elsewhere [33, 34, 35].

The data acquisition rate of indirect detector systems can be pushed up the range of $> 10^4$ images/s (i. e. tens of µs/image) when CMOS cameras are used instead of CCDs [36, 37]. The higher data acquisition speed of CMOS cameras is only compromised by the limited dynamic range as well as the short exposure times required. To some extent, frame transfer CCD cameras represent up to now a compromise between CCD and CMOS cameras [28].

The crucial component of any indirect detector which defines its performance in terms of efficiency as well as resolution in space and time is the luminescence screen. For this reason, a lot of effort has been put into developing optimised scintillator material compositions for synchrotron-based microimaging applications [38, 39, 40, 41, 42, 43, 44].

III. *IN VIVO* CINERADIOGRAPHY

In medical terminology, cineradiography is the technique of making motion pictures with X-rays (radiographs) either for research or medical diagnostics. In this article, the extension of digital radiography to time-resolved imaging of living organisms is called *in vivo* cineradiography. It can be considered an advancement of Lucien Bull's work: from visible light to the use of hard X-rays.

As an application, the study of the biting and chewing mouthparts of the cockroach *Periplaneta americana* (Linné) is shown. Cockroaches are adequate model organisms for studying basic insect chewing coordination and function due to their rather primitive mouthparts. Descriptive studies of the kinematics of the entire mouthpart are challenging due to an overlap of the involved opaque objects. From previous studies it is known that synchrotron-based hard X-ray microimaging combined with inline X-ray phase contrast allows for *in vivo* cineradiography of insects [45, 46, 47, 48]. The latter were all performed with monochromatic radiation using double-crystal monochromators at the Advanced Photon Source (Chicago, USA). The potential of white beam inline X-ray phase contrast is known as well, but was not employed so far for cineradiography [49, 50].

The measurements were carried out at the beamline TopoTomo of the German synchrotron light source ANKA [51], which is fed by a 1.5 T bending magnet (critical energy of 6.2 keV, 2.5 GeV ring energy) [52, 53, 54]. TopoTomo can be run in the white beam mode, using only a single 0.5-mm thick Be-window between the experimental station and the source. The 30 m-long source-to-sample distance and the source size of 0.5 mm × 0.14 mm (h × v, FWHM) are well suited to perform microimaging with X-ray phase contrast. For the measurements, TopoTomo was operated in the white beam mode with the polychromatic radiation being additionally filtered by 1 mm Si after passing the Be-window. The peak photon flux density of the resulting spectrum is around 20 keV, the integral photon flux density of the order of 10^{11} Ph/s/mm^2 [54]. As detector, the so-called BAM*line* macroscope was used [55]: Rodenstock right-angle objectives (focal length f = 50 mm and 122 mm available) in combination with a Nikkor 180/2.8 ED (f = 180 mm) as tube lens (similar to Fig 1, left). As scintillator screen, bulk $CdWO_4$ (CWO) or Ce-doped $(LuY)_2SiO_5$ (LYSO:Ce) single crystals were applied [56, 57]. The camera used to capture the luminescence image of the scintillator via the visible light optics with high speed was a Photron Fastcam SA1 [58]. The SA1 is based on a 1024 × 1024 pixel CMOS chip, 20 µm pixel size

(peak quantum efficiency of 42% at 640 nm). The dynamic range is 10bit (800:1) with a 12bit digitalization. The minimal shutter time is 2 µs and can be triggered with 100 ns time resolution. Without restricting the region-of-interest (ROI) the camera can acquire 5 400 images per second, with a reduced ROI up to 675 000 images/s (64 × 16 pixel). 32 GB on-board memory are installed for a fast intermediate data storage. In order to fully exploit the advantages of inline phase contrast, this X-ray detector was positioned approximately 0.5 m from the specimen.

In Fig. 2, example images extracted from a movie showing a feeding cockroach are displayed. They were taken with a frame acquisition rate of 125 images/s. The detector was equipped with a bulk LYSO:Ce crystal. The effective pixel size was around 13.5 µm (resulting in a real spatial resolution around 30 µm applying Shannon's theorem). The full movie is available online [59]. Due to the hard spectrum employed, the contrast is dominated by refraction (phase contrast). The time resolution is sufficient to sample one chewing cycle with about 40 images. Relaxing the demands on spatial resolution and/or signal-to-noise ratio allows one to reach even higher data acquisition rates. Movies with 250 images/s were taken during the same experiment as well [60]. In principle, the imaging speed is only limited by the dose the living specimen can stand. Hence, frame rates up to 1 000 images are imaginable.

Employing polychromatic radiation is a valuable option in order to perform *in vivo* cineradiography at synchrotron light sources where the available photon flux density is not high enough to use monochromatic radiation. Despite the large energy spread, refraction by means of inline X-ray phase contrast is available. One of the drawbacks is the higher dose involved.

IV. *IN SITU* MICRORADIOSCOPY

In materials research, samples can often stand a higher dose than in life sciences. Thus, higher frame rates or other contrast modes can be applied in microradioscopy. In the previous chapter, the high imaging speed was accessible despite the moderate available photon density due to the use of X-ray inline phase contrast that is more sensitive and therefore less demanding on flux. More photons are needed in order to achieve comparable contrast and frame rates when absorption information is required.

In this section, the visualization of semi-solid metal flow at an acquisition rate of 500 images/s is shown. Semi-solid casting (SSC) is an experimental production process for light metals, currently in use for niche-market applications only. It leads to a reduction of unwanted shrinkage during solidification due to the lower processing temperatures [61]. The process holds promise of improved mechanical properties at only slightly higher costs. Until now, SSC is preferably applied to coarse structures: it suffers from the incomplete understanding of the rheological properties of the metallic two-phase mixture. More knowledge would be necessary for numerical simulations and an optimization of the process. Particularly for thin cavities of dimensions close to the average particle / cluster size of the solid-phase, SSC yields only poor results. *In situ* microradioscopy now provides a tool for visualizing injection processes in such cavities directly.

Images were taken at the high-flux beamline ID15a of the European Synchrotron Radiation Facility (ESRF) [28]. As X-ray source, the available asymmetric multipole wiggler (1.84 T, 44 keV critical energy) was chosen. Further details on the beamline are available online [62]. The white radiation was filtered with approximately 20 mm of silicon, the photon flux density available for the imaging experiment is estimated to 10^{15} Ph/s/mm^2. The employed detector system is an ESRF in-house development, similar to the design shown in Fig 1 (right): a manual zoom objective in combination with a lens projects the scintillator image through a lead glass and a mirror onto the camera. The system has been successfully used for high speed imaging earlier [36]. As scintillator, a 100 µm-thick YAG:Ce (Ce-doped $Y_3Al_5O_{12}$) single crystal was chosen [41]. The camera was again the Photron Fastcam SA1 (see previous section for technical details). Images were acquired at 500 frames/s and 5.5 µm effective pixel size (spatial resolution R > 11 µm). Since the readout time of the CMOS chip is negligibly short, each frame corresponds to an exposure of 2 ms. The distance between the sample and the detector was approximately 0.1 m (closest possible distance in order to reduce phase contrast effects).

An experimental setup for *in situ* flow monitoring of semi-solid slurry was constructed by the Helmholtz Zentrum Berlin für Materialien und Energie GmbH and the Federal Institute for Materials Research and Testing (BAM), both Germany. A detailed description has been published elsewhere [63, 64]. After heating the Al-32Ge alloy to 450°C, a miniaturized injection process was captured with the high-speed imaging system, see Fig. 3. Semi-solid slurry was pushed through a 0.4 mm thin bottleneck by a steel piston advancing at a speed

of v = 2 cm/s.

Fig. 3 displays four radiographs showing the injection into the bottleneck (a-d): from the movie taken, pictures are shown in intervals of 100 images (corresponding to 0.2 s), each of them with an exposure time of 2 ms. The gray values represent a density / atomic number contrast between three phases: air (black), liquid melt (bright gray) and solid particles (dark gray). First, we observe the liquid entering the channel and filling the recipient. Meanwhile solid particles and particle clusters detach from the solid bulk and follow the liquid flow into the cavity at high speed. Few particles / clusters remain close to the liquid-air interface while most particles which traverse the bottleneck move through the melt. During the experiment, small air bubbles appear in the liquid as black spherical objects and disappear soon after their emergence, possibly due to dissolution of the gases in the melt. Once the recipient has been filled with liquid and some solid particles / clusters the flow stops. The remaining solid feedstock can no longer traverse the channel and the down-driving piston is seen to compact the particles to a dense aluminum-rich matrix (top of Fig. 3d). Optical flow analysis can then be used to calculate the two-dimensional displacements between two consecutive X-ray images [60, 64].

V. RADIOSCOPY WITH SPATIO-TEMPORAL MICRORESOLUTION

In order to observe fast processes which last only a few milliseconds even higher imaging speeds with exposure times in the microsecond range are required. Events in liquid foams such as coalescence and cell wall collapse fall into that category [37, 65, 66, 67]. Reaching a data acquisition rate that implies taking several thousand images per second requires the combination of high photon flux density with white beam inline X-ray phase contrast imaging.

As an example, the study of a single coalescence event in a liquid metal foam is shown, see Fig. 4. Images were again taken at the ESRF beamline ID15a [28, 62]. This time, the applied ESRF in-house designed detector optic consisting of a single objective with a fixed focal length captures the luminescence image of the scintillator without magnification via a mirror [27]. As scintillator screen, 200-µm thick bulk LuAG:Ce (Ce-doped $Lu_3Al_5O_{12}$) was chosen due to its high stopping power and light yield as well as resistance to heat load [28, 41]. The camera was again the Photron SA1 (see section III for technical details

on the camera), operated with a restricted region-of-interest to reach frame rates above 10 000 images/s. The white radiation of the source was filtered by approximately 25 mm of silicon. The sample-to-detector distance was increased to around 0.5 m in order to fully exploit phase contrast.

The foaming of AlSi6Cu4 was carried out under 5 bar argon pressure in a furnace at 600°C as described earlier [36]. The furnace was depressurized during expansion in order to increase rapidly the foam volume and therefore the growth-induced cell wall rupture rate during the short time window in which the camera can save images at the high frame rate. The coalescence event shown in Fig. 4 was captured by taking 40 000 images/s (the complete movie is available online [69]). The entire merger of two pores happens here within around 3 ms, sampled in time with 120 images. The main features displayed in Fig. 4 are: at 0 µs two pores and the joint cell wall are still distinguishable, 450 µs later, the cell wall has ruptured, but still the original shape of the two pores is visible. Then, at 750 µs the new walls are already straight – defining the so-called rupture time [36]. After 3.4 ms, oscillations of the new cell walls have stopped. We note that the coalescence event could be resolved due to the high spatio-temporal resolution used. Nevertheless, the rupture of the cell wall itself is not resolved, the specific wall between the two pores rather seems to disappear suddenly between frame 17 (400 µs) and 18 (425 µs).

Time-resolved studies like the one introduced are important to extend the knowledge about the effective viscosity of liquid metal in a cell wall and the mechanisms behind foam stability [68, 70, 71]. The rupture time measured allows one to conclude that the collapse of this single cell wall is dominated by inertia. Hence, modifying, e. g., the viscosity of the liquid melt should have only minor influence.

VI. TIME-RESOLVED MICROTOMOGRAPHY

In order to extend radiography towards tomography, several hundred projection images have to be recorded. This naturally reduces the imaging rates by orders of magnitude when progressing from two to three dimensions. Nevertheless, processes like, e. g., corrosion or hardening can occur on time-scales which would allow for three-dimensional investigations using these tomographic imaging rates. First approaches to access higher imaging speeds for synchrotron-based hard X-ray microtomography by employing radiation with a larger

energy spread reach back to the beginning of this century [72]. While with monochromatic radiation it has been demonstrated that scanning times of a few minutes down to less than half a minute are applicable [73, 74], the use of white high-energy synchrotron radiation could allow one to acquire tomographic data sets within only a few seconds [28]. More recently, successful experiments have been reported which combine, e. g., monochromatic undulator radiation or polychromatic radiation from so-called super-bends with fast detectors, in order to study the evolution of two-constituent specimens by taking tomographic data sets within a few seconds down to less than 1 s [75, 76, 77, 78].

As a feasibility study, a static sample made of concrete (kindly provided by Prof. Konietzky, TU Bergakademie Freiberg, Germany) was scanned with similar parameters as chosen in paragraph IV: the white beam of the ESRF beamline ID15a was filtered with 25 mm of silicon. The ESRF in-house designed zoom optic with 1.5x effective magnification was combined with the Photron SA1 camera (13.3 µm effective pixel size). As scintillator, a 200-µm thick YAG:Ce crystal was chosen. The available rotation stage was operated in a kind of infinite loop with a rotation speed of 45°/s. Triggering of the camera by the rotation stage was not applied. The Photron camera acquired 250 images/s which resulted in a utilization of approximately 80% of the camera's dynamic range. Thus, an entire tomographic scan with a 180° rotation, sampled with 1000 projection images was acquired in 4 s. The resulting tomographic reconstruction of one selected slice is shown in Fig. 5. Inside this multi-constituent specimen, a highly absorbing impurity is discernable next to pores inside the matrix.

VII. SUMMARY

The polychromatic hard X-ray radiation of a third-generation synchrotron bending magnet or insertion device delivers a photon flux density high enough to perform time-resolved radiography. Depending on the available number of photons as well as the desired signal-to-noise-ratio and resolution in space and time, imaging rates from a few hundred frames per second up to several 10 000 frames per second can be reached. Existing indirect X-ray image detectors can be combined with commercially available CMOS cameras, which allows for a high data acquisition rate. Selected applications from life sciences (*in vivo* cineradiography) and materials research (*in situ* microradioscopy) demonstrate the high potential of

this technique.

Besides the high photon flux density, another advantage of synchrotron light sources is the partial coherence of the X-ray wave front at the position of the experiment. Hence, interference effects can be used to access more sensitive contrast modalities such as the inline X-ray phase contrast. The increased sensitivity allows one compensating a moderate photon flux density or accessing even higher data acquisition rates in specific cases. The amount of photons available at high-flux beamlines like ID15a of the European Synchrotron Radiation Facility should be sufficient to reach data rates above 100 000 images/s. Currently, the limiting factor is the scintillator screen that usually does not stand the corresponding high heat load: cracks lead to irreversible damage.

Such high frame rates will allow us to reach higher acquisition rates in synchrotron-based microtomography as well, allowing one to study processes in three dimensions with a high time resolution. Microtomography with high spatial resolution as well as good contrast is commonly performed at synchrotron light sources with monochromatic radiation and by applying CCD cameras with a high dynamic range, like, e. g., the ESRF in-house development FReLoN [79]. Despite their limited dynamic range, current CMOS cameras can be applied to a certain extent to time-resolved microtomography of multi-constituent specimens. In the future, novel developments like the so-called scientific CMOS chips might open further new opportunities [80].

Acknowledgments

We acknowledge T. Martin, C. Jarnias, M. Peele, M. Di Michiel, V. Honkimäki, T. Weitkamp (ESRF), A. Dieterich, L. Körner (Universität Tübingen), D. Haas, T. dos Santos Rolo, L. Helfen, T. Baumbach, H. Schade, A. Volker (ANKA), for all the support and fruitful discussions, Prof. Konietzky (TU Bergakademie Freiburg) for the concrete sample. W. Tutsch (PCO AG, Germany) and A. Bridges (Photron Inc., USA) enlightened us with details about CMOS cameras.

---

[1] D. Smith. A case study and analysis of the Tacoma narrows bridge failure. Engineering Project 99.497, Department of Mechanical Engineering, Carleton University, Ottawa, Canada, March

1974.

[2] Y. Billah and B. Scanlan. Resonance, Tacoma narrows bridge failure, and undergraduate physics textbooks. *Am. J. Phys.*, 59(2):118–124, 1991.

[3] L. Bull. *La Cinématographie*. Paris: Armand Collin, 1928.

[4] N. Kardjilov, A. Hilger, I. Manke, M. Strobl, W. Treimer, and J. Banhart. Industrial applications at the new cold neutron radiography and tomography facility of the HMI. *Nucl. Instr. Meth. A*, 542:16–21, 2005.

[5] Y. Wang, X. Liu, K.-S. Im, W.-K. Lee, J. Wang, K. Fezzaa, D. L. S. Hung, and J. R. Winkelman. Ultrafast X-ray study of dense-liquid-jet flow dynamics using structure-tracking velocimetry. *Nat. Phys.*, 4(4):305–309, 2008.

[6] P. Cloetens, R. Barrett, J. Baruchel, J.-P. Guigay, and M. Schlenker. Phase objects in synchrotron radiation hard X-ray imaging. *J. phys. D: Appl. phys.*, 29(1):133–146, 1996.

[7] K. A. Nugent, T. E. Gureyev, D. F. Cookson, D. Paganin, and Z. Barnea. Quantitative phase imaging using hard X rays. *Phys. Rev. Lett.*, 77:2961–2964, 1996.

[8] A. Snigirev, I. Snigireva, V. Kohn, and S. Kuznetsov. On the possibilities of X-ray phase contrast microimaging by coherent high-energy synchrotron radiation. *Rev. Sci. Instrum.*, 66(12):5486–5492, 1995.

[9] W. Graeff and K. Engelke. Microradiography and microtomography. In S. Ebashi, M. Koch, and E. Rubenstein, editors, *Handbook on Synchrotron Radiation*, volume 4, pages 361–406. North-Holland; Amsterdam, Oxford, New York, Tokyo, 1991.

[10] J. Banhart, editor. *Advanced Tomographic Methods in Materials Research and Engineering*. Oxford University Press, 2008.

[11] J.-I. Chikawa and I. Fujimoto. X-ray diffraction topography with a Vidicon television image system. *Appl. Phys. Lett.*, 13(11):387–389, 1968.

[12] W. Hartmann, G. Markewitz, U. Rettenmaier, and H. J. Queisser. High resolution direct-display X-ray topography. *Appl. Phys. Lett.*, 27:308–309, 1975.

[13] T. Tuomi, V. Kelhä, and M. Blomberg. Real-time video imaging of synchrotron X-ray topographs: Moving multiple diffraction stripes. *Nucl. Instr. & Meth.*, 208:697–700, 1983.

[14] R. K. Swank. Calculation of modulation transfer functions of X-ray fluorescent screens. *Appl. Optics*, 12(8):1865–1870, 1973.

[15] A. Koch, C. Raven, P. Spanne, and A. Snigirev. X-ray imaging with submicrometer resolution

employing transparent luminescent screens. *J. Opt. Soc. Am.*, 15:1940–1951, 1998.

[16] E. Spiller. Recent developments towards high resolution X-ray imaging. *Nucl. Instr. & Meth.*, 177(1):187–192, 1980.

[17] J. C. Elliott and S. D. Dover. X-ray microtomography. *J. Microsc.*, 126(2):211–213, 1982.

[18] A. C. Thompson, J. Llacer, L. Campbell Finman, E. B. Hughes, J. N. Otis, S. Wilson, and H. D. Zeman. Computed tomography using synchrotron radiation. *Nucl. Instr. Meth.*, 222(1–2):319–323, 1984.

[19] D. K. Bowen, J. C. Elliott, S. R. Stock, and S. D. Dover. X-ray microtomography with synchrotron radiation. In D. K. Bowen and L. V. Knight, editors, *X-ray imaging II*, volume 691 of *Proc. of SPIE*, pages 94–98, 1986.

[20] B. P. Flannery, H. W. Deckmann, W. G. Roberge, and K. L. D'Amico. Three-dimensional X-ray microtomography. *Science*, 237(4821):1439–1444, 1987.

[21] P. Spanne and M. L. Rivers. Computerized microtomography using synchrotron radiation from the NSLS. *Nucl. Instrum. & Meth. Phys. Res. B*, 24-25:1063–1067, 1987.

[22] J. H. Kinney, Q. C. Johnson, M. C. Nichols, U. Bonse, R. A. Saroyan, R. Nusshardt, and R. Pahl. X-ray microtomography on beamline X at SSRL. *Rev. Sci. Instrum.*, 60(7):2471–2474, 1989.

[23] J. H. Kinney, Q. C. Johnson, U. Bonse, R. Nusshardt, and M. C. Nichols. The performance of CCD array detectors for application in high-resolution tomography. In D. K. Bowen and L. V. Knight, editors, *X-ray imaging II*, volume 691 of *Proc. of SPIE*, pages 43–50, 1986.

[24] U. Bonse, R. Nusshardt, F. Busch, R. Pahl, Q. C. Johnson, J. H. Kinney, R. A. Saroyan, and M. C. Nichols. Optimization of CCD-based energy-modulated X-ray microtomography. *Rev. Sci. Instrum.*, 60(7):2478–2481, 1989.

[25] J. P. Henry, E. M. Kellogg, U. G. Briel, S. S. Murray, and L. P. Van Speybroeck. High resolution X-ray imaging detector for astronomical measurements. In D. K. Bowen and L. V. Knight, editors, *X-ray imaging II*, volume 691 of *Proc. of SPIE*, pages 43–50, 1986.

[26] U. Bonse and F. Busch. X-ray computed microtomography (μCT) using synchrotron radiation (SR). *Prog. Biophys. Molec. Biol.*, 65:133–169, 1996.

[27] A. Koch. Lens coupled scintillating screen-CCD X-ray area detector with a high quantum efficiency. *Nucl. Instrum. & Meth. in Phys. Res. A*, 348:654–658, 1994.

[28] M. Di Michiel, J. M. Merino, D. Fernandez-Carreiras, T. Buslaps, V. Honkimäki, P. Falus,

T. Martins, and O. Svensson. Fast microtomography using high energy synchrotron radiation. *Rev. Sci. Instrum.*, 76:043702–1–043702–7, 2005.

[29] S. Koerner, B. Schillinger, P. Vontobel, and H. Rauch. A neutron tomography facility at a low power research reactor. *Nucl. Instr. Meth. A*, 471(1–2):69–74, 2001.

[30] Y. Wang, F. De Carlo, D. C. Mancini, I. McNulty, B. Tieman, J. Bresnahan, I. Foster, J. Insley, P. Lange, G. von Laszewski, C. Kesselmann, M.-H. Su, and M. Thibaux. A high-throughput X-ray microtomography system at the Advanced Photon Source. *Rev. Sci. Instrum.*, 72(4):2062–2068, 2001.

[31] A. Danilewsky, J. Wittge, A. Hess, A. Cröll, D. Allen, P. McNally, P. Vagovic, A. Cecilia, Z. Li, T. Baumbach, E. Gorostegui-Colinas, and M. R. Elizalde. Dislocation generation related to micro-cracks in Si wafers: High temperature in situ study with white beam X-ray topography. *Nucl. Instr. Meth. B*, 268(3–4):399–402, 2010.

[32] A. N. Danilewsky, J. Wittge, A. Rack, T. Weitkamp, R. Simon, and P. McNally. White beam topography of 300 mm Si-wafers. *J. Mater. Sci.: Mater. Electron.*, 19:269–272, 2008.

[33] H. Graafsma and T. Martin. Detectors for synchrotron tomography. In J. Banhart, editor, *Advanced Tomographic Methods in Materials Research and Engineering*, pages 277–302. Oxford University Press, 2008.

[34] S. M. Gruner, M. W. Tate, and E. F. Eikenberry. Charge-coupled device area X-ray detectors. *Rev. Sci. Instrum.*, 73:2815–2842, 2002.

[35] M. J. Renzi, M. W. Tate, A. Ercan, S. M. Gruner, E. Fontes, C. F. Powell, A. G. Mac-Phee, S. Narayanan, J. Wang, Y. Yue, and R. Cuenca. Pixel array detectors for time resolved radiography. *Rev. Sci. Instrum.*, 73:1621–1624, 2002.

[36] F. García-Moreno, A. Rack, L. Helfen, T. Baumbach, S. Zabler, N. Babcsán, J. Banhart, T. Martin, C. Ponchut, and M. Di Michiel. Fast processes in liquid metal foams investigated by high-speed synchrotron X-ray microradioscopy. *Appl. Phys. Lett.*, 92:134104–1–134104–3, 2008.

[37] A. Rack, F. García-Moreno, T. Baumbach, and J. Banhart. Synchrotron-based radioscopy employing spatio-temporal micro-resolution for studying fast phenomena in liquid metal foams. *J. Synchrotron Radiat.*, 16(3):432–434, 2009.

[38] P. A. Rodnyi. *Physical Processes in Inorganic Scintillators*. CRC Press, Boca Raton; New York, 1997.

[39] A. Koch, F. Peyrin, P. Heurtier, B. Ferrand, B. Chambaz, W. Ludwig, and M. Couchaud. X-ray camera for computed microtomography of biological samples with micrometer resolution using $Lu_3Al_5O_{12}$ and $Y_3Al_5O_{12}$ scintillators. In J. M. Boone and J. T. Dobbins III, editors, *Physics of Medical Imaging*, volume 3659 of *Proc. of SPIE*, pages 170–179, 1999.

[40] T. Martin and A. Koch. Recent developments in X-ray imaging with micrometer spatial resolution. *J. Synchrotron Rad.*, 13:180–194, 2006.

[41] J. Touš, M. Horváth, L. Pína, K. Blažek, and B. Sopka. High-resolution application of YAG:Ce and LuAG:Ce imaging detectors with a CCD X-ray camera. *Nucl. Instr. & Meth. Res. A*, 591:264–267, 2008.

[42] T. Martin, P.-A. Douissard, M. Couchaud, A. Cecilia, T. Baumbach, K. Dupré, and A. Rack. LSO-based single crystal film scintillator for synchrotron-based hard X-ray micro-imaging. *IEEE Trans. Nucl. Sci.*, 56(3):1412–1416, 2009.

[43] A. Cecilia, A. Rack, D. Pelliccia, P.-A. Douissard, T. Martin, M. Couchaud, K. Dupré, T. Baumbach. Studies of LSO:Tb radio-luminescence properties using white beam hard X-ray synchrotron irradiation. *Rad. Eff. Def. Solids*, 164(9):517–522, 2009.

[44] P.-A. Douissard, A. Cecilia, T. Martin, V. Chevalier, M. Couchaud, T. Baumbach, K. Dupré, M. Kühbacher, and A. Rack. Novel epitaxially grown LSO-based thin film scintillator for micro-imaging using hard synchrotron radiation. *J. Synchrotron Radiat.*, 17(5): in print, 2010.

[45] M. W. Westneat, O. Betz, R. W. Blob, K. Fezzaa, W. J. Cooper, and W.-K. Lee. Tracheal respiration in insects visualized with synchrotron X-ray imaging. *Science*, 299:558–560, 2003.

[46] J. J. Socha, M. W. Westneat, J. F. Harrison, J. S. Waters, and W.-K. Lee. Real-time phase-contrast X-ray imaging: a new technique for the study of animal form and function. *BMC Biology*, 5(1):6, 2007.

[47] M. W. Westneat, J. J. Socha, and W.-K. Lee. Advances in biological structure, function, and physiology using synchrotron X-ray imaging. *Annu. Rev. Physiol.*, 70:119–142, 2008.

[48] B. J. Sinclair, A. G. Gibbs, W.-K. Lee, A. Rajamohan, S. P. Roberts, and J. J. Socha. Synchrotron X-ray visualisation of ice formation in insects during lethal and non-lethal freezing. *PLoS ONE*, 4(12):e8259, 12 2009.

[49] A. G. Peele, F. De Carlo, P. J. McMahon, B. B. Dhal, and K. A. Nugent. X-ray phase contrast tomography with a bending magnet source. *Rev. Sci. Instrum.*, 76(8):083707, 2005.

[50] V. G. Kohn, T. S. Argunova, and J. H. Je. Study of micropipe structure in SiC by X-ray phase contrast imaging. *Appl. Phys. Lett.*, 91(17):171901, 2007.

[51] H. O. Moser. New synchrotron radiation facility ANKA at Karlsruhe. *J. Alloy. Compd.*, 328:42–49, 2001.

[52] A. N. Danilewsky, R. Simon, A. Fauler, M. Fiederle, and K. W. Benz. White beam X-ray topography at the synchrotron light source ANKA, Research Centre Karlsruhe. *Nucl. Instr. Meth. B*, 199:71–74, 2003.

[53] A. N. Danilewsky, A. Rack, J. Wittge, T. Weitkamp, R. Simon, H. Riesemeier, and T. Baumbach. White beam synchrotron topography using a high resolution digital X-ray imaging detector. *Nucl. Instrum. & Meth. in Phys. Res. B*, 266:2035–2040, 2008.

[54] A. Rack, T. Weitkamp, S. Bauer Trabelsi, P. Modregger, A. Cecilia, T. dos Santos Rolo, T. Rack, D. Haas, R. Simon, T. Baumbach, R. Heldele, M. Schulz, B. Mayzel, A. N. Danilewsky, T. Waterstradt, W. Diete, H. Riesemeier, B. R. Müller, and T. Baumbach. The micro-imaging station of the TopoTomo beamline at the ANKA synchrotron light source. *Nucl. Instr. Meth. B*, 267(11):1978–1988, 2009.

[55] A. Rack, S. Zabler, B.R. Müller, H. Riesemeier, G. Weidemann, A. Lange, J. Goebbels, M. Hentschel, and W. Görner. High resolution synchrotron-based radiography and tomography using hard X-rays at the BAMline (BESSY II). *Nucl. Instr. Meth. A*, 586(2):327–344, 2008.

[56] L. Nagornaya, G. Onyshchenko, E. Pirogov, N. Starzhinskiy, I. Tupitsyna, V. Ryzhikov, Y. Galich, Y. Vostretsov, S. Galkin, and E. Voronkin. Production of the high-quality CdWO4 single crystals for application in CT and radiometric monitoring. *Nucl. Instrum. & Meth. in Phys. Res. A*, 537:163–167, 2005.

[57] I. G. Valais, I. S. Kandarakis, A. Konstantinidis, D. N. Nikolopoulos, I. Sianoudis, D. A. Cavouras, N. Dimitropoulos, C. D. Nomicos, and G. S. Panayiotakis. Evaluation of the light emission efficiency of LYSO:Ce scintillator under X-ray excitation for possible applications in medical imaging. *Nucl. Instr. & Meth. in Phys. Res. A*, 569:201–204, 2006.

[58] T. Inoue, S. Takeuchi, and S. Kawahito. CMOS active pixel image sensor with in-pixel CDS for high-speed cameras. In Dennis L. Paisley, Stuart Kleinfelder, Donald R. Snyder, and Brian J. Thompson, editors, *High-Speed Solid State Sensors and Circuits II*, volume 5580 of *Proc. of SPIE*, pages 293–300, 2005.

[59] http://www.alexanderrack.eu/cockroach_movie.avi, last visit 2010.

[60] O. Betz, A. Rack, C. Schmitt, A. Ershov, A. Dieterich, L. Körner, A. Ershov, and T. Baumbach. High-speed X-ray cineradiography for analyzing complex kinematics in living insects. *Synchrotron Rad. News*, 21(5):34–38, 2008.

[61] M. C. Flemings. Behavior of metal alloys in the semisolid state. *Metall. Trans. A*, 22(5):957–981, 1991.

[62] *ID15 High Energy Diffraction and Scattering Beamlines.* http://www.esrf.eu/UsersAndScience/Experiments/StructMaterials/ID15, last visit 2010.

[63] S. Zabler, A. Rueda, A. Rack, H. Riesemeier, P. Zaslansky, I. Manke, F. García-Moreno, and J. Banhart. Coarsening of grain-refined semi-solid Al-Ge32 alloy: X-ray microtomography and in situ radiography. *Acta Mater.*, 55(15):5045–5055, 2007.

[64] S. Zabler, A. Rack, A. Rueda, L. Helfen, F. García-Moreno, and J. Banhart. Direct observation of particle flow in semi-solid alloys by synchrotron X-ray micro-radioscopy. *Physica stat. sol. A*, 207(3):718–723, 2010.

[65] B. M. Weon, J. H. Je, Y. Hwu, and G. Margaritondo. Decreased surface tension of water by hard-X-ray irradiation. *Phys. Rev. Lett.*, 100(21):217403, May 2008.

[66] J. Banhart, H. Stanzick, L. Helfen, and T. Baumbach. Metal foam evolution studied by synchrotron radioscopy. *Appl. Phys. Lett.*, 78(8):1152–1154, 2001.

[67] S. Ata, E. S. Davis, D. Dupin, S. P. Armes, and E. J. Wanless. Direct observation of ph-induced coalescence of latex-stabilized bubbles using high-speed video imaging. *Langmuir*, 26(11):7865–7874, 2010.

[68] A. Myagotin, L. Helfen, and T. Baumbach. Coalescence measurements for evolving foams monitored by real-time projection imaging. *Meas. Sci. Technol.*, 20(5):055703, 2009.

[69] http://www.alexanderrack.eu/coalescence_movie.avi, last visit 2010.

[70] A. Rack, H.-M. Helwig, A. Bütow, A. Rueda, B. Matijašević-Lux, L. Helfen, J. Goebbels, and J. Banhart. Early pore formation in aluminium foams studied by synchrotron-based microtomography and 3-D image analysis. *Acta Mater.*, 57(16):4809–4821, 2009.

[71] A. Haibel, A. Rack, and J. Banhart. Why are metal foams stable? *Appl. Phys. Lett.*, 89(15):154102, 2006.

[72] C. Rau, T. Weitkamp, A. A. Snigirev, C. G. Schroer, B. Benner, J. Tuemmler, T. F. Guenzler, M. Kuhlmann, B. Lengeler, C. E. Krill III, K. Doebrich, D. Michels, and A. Michels. Tomog-

raphy with high resolution. In Ulrich Bonse, editor, *Developments in X-Ray Tomography III*, volume 4503 of *Proc. of SPIE*, pages 14–22, 2002.

[73] P. Babin, G. Della Valle, H. Chiron, P. Cloetens, J. Hoszowska, P. Pernot, A. L. Réguerre, L. Salvo, and R. Dendievel. Fast X-ray tomography analysis of bubble growth and foam setting during breadmaking. *J. Cereal Sci.*, 43(3):39–397, 2006.

[74] J. Lambert, I. Cantat, R. Delannay, A. Renault, F. Graner, J. A. Glazier, I. Veretennikov, and P. Cloetens. Extraction of relevant physical parameters from 3D images of foams obtained by X-ray tomography. *Colloids Surf. A*, 263(1–3):295–302, 2005.

[75] K. Uesugi, T. Sera, and N. Yagi. Fast tomography using quasi-monochromatic undulator radiation. *J. Synchrotron Radiat.*, 13(5):403–407, 2006.

[76] H. Takano, K. Yoshida, T. Tsuji, T. Koyama, Y. Tsusaka, and Y. Kagoshima. Fast X-ray micro-CT for real-time 4D observation. *J. Phys.: Conf. Series (XRM2008)*, 186:012049, 2009.

[77] A. Momose, W. Yashiro, H. Maikusa, and Y. Takeda. High-speed X-ray phase imaging and X-ray phase tomography with Talbot interferometer and white synchrotron radiation. *Opt. Express*, 17(15):12540–12545, 2009.

[78] R. Mokso, F. Marone, and M. Stampanoni. Real time tomography at the Swiss Light Source. In R. Garrett, I. Gentle, K. Nugent, and S. Wilkins, editors, *AIP Conference Proceedings (SRI09)*, volume 1234, pages 87–90, 2010.

[79] J.-C. Labiche, O. Mathon, S. Pascarelli, M. A. Newton, G. G. Ferre, C. Curfs, G. Vaughan, A. Homs, and D. F. Carreiras. The fast readout low noise camera as a versatile X-ray detector for time resolved dispersive extended X-ray absorption fine structure and diffraction studies of dynamic problems in materials science, chemistry, and catalysis. *Rev. Sci. Instrum.*, 78:0901301, 2007.

[80] G. Holst. Scientific CMOS image sensors. *Laser+Photonics*, 5:18–21, 2009.

APPENDIX A: FIGURES

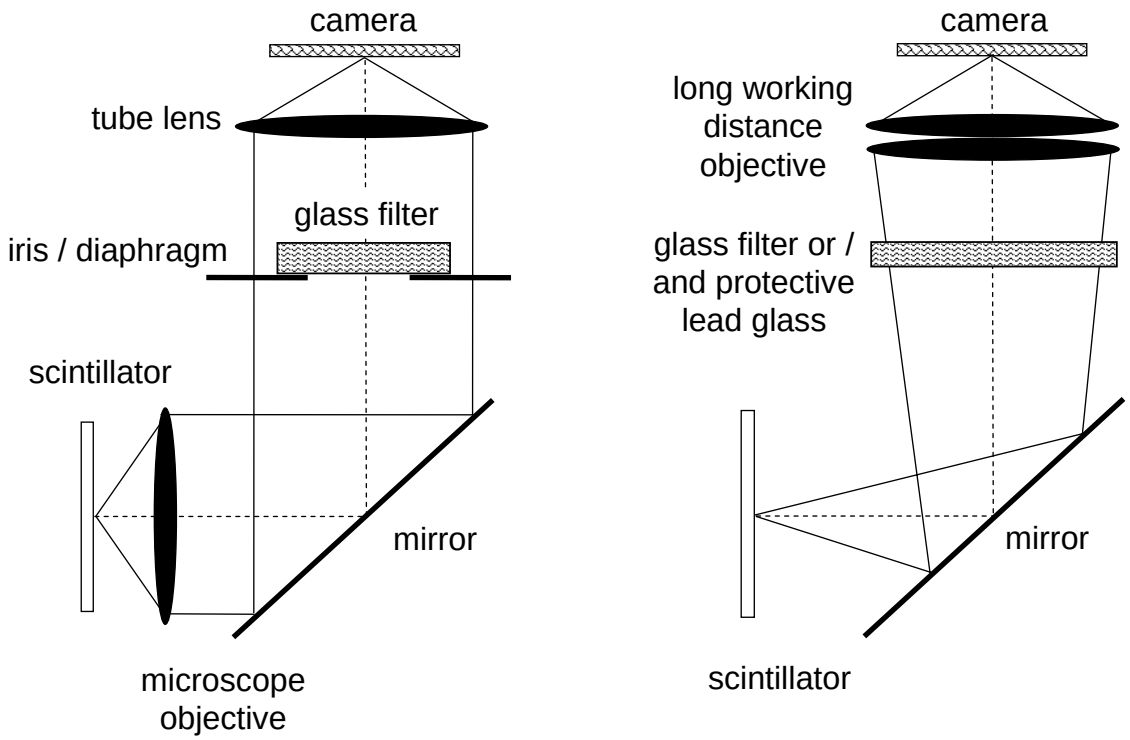

FIG. 1: The two main designs that emerged for high resolution indirect X-ray image detection in the past decades, using either a visible-light microscope with a folded beam path (left [26]) or a long working distance objective (right [12, 27]) to project the luminescence image of a scintillator screen onto a camera.

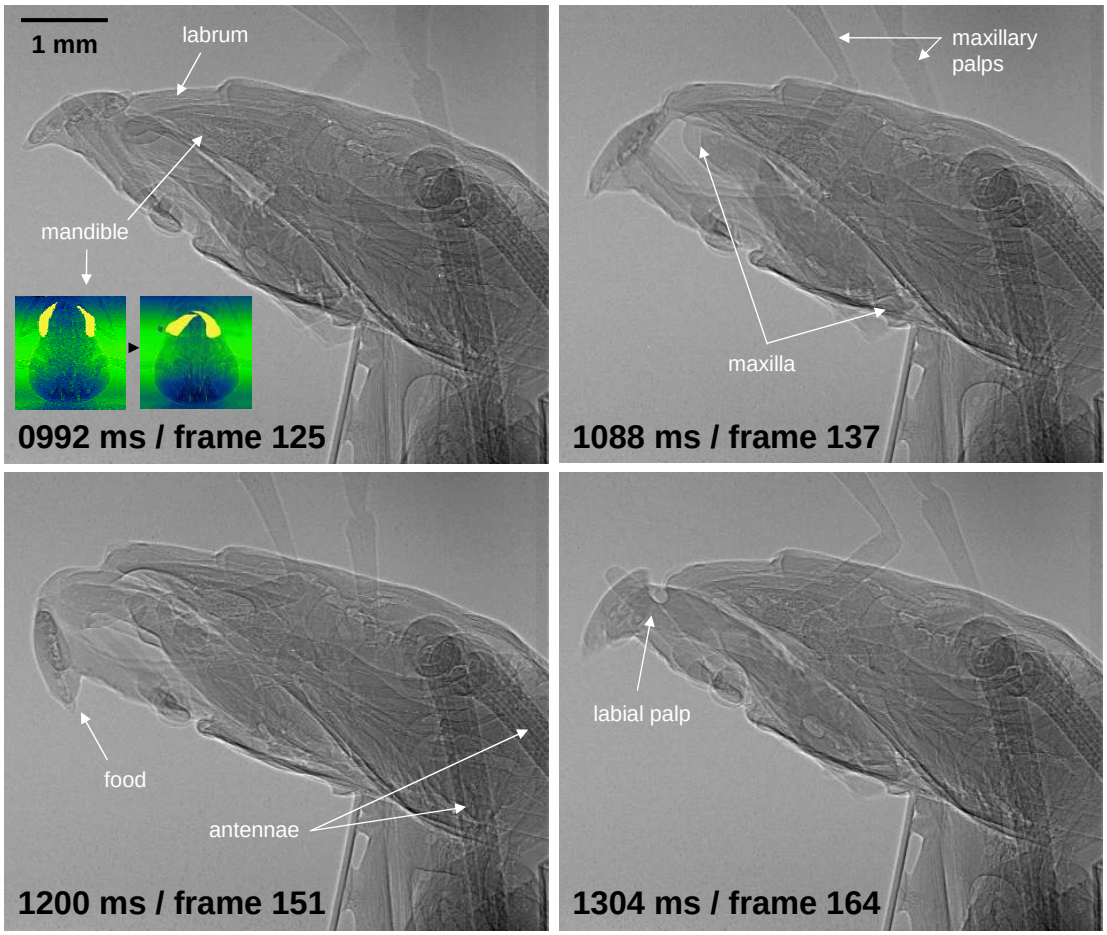

FIG. 2: Sequence of four consecutive *in vivo* images showing the head of Periplaneta americana during ingestion (acquired at the TopoTomo beamline of the ANKA light source, Germany). Due to the lateral perspective the multilayered assembly can easily be understood (from dorsal to ventral: labrum, mandibles, maxillae and labium). During food intake these mouthparts interact in a periodic way (see movie sequence deposited online [59]). The small inset pictures in the upper left quarter illustrate the position of the mandibles (highlighted in yellow) as can be seen in the dorsal view. The movie was acquired with 125 images/s data acquisition speed. The effective pixel size is approximately 13.5 µm.

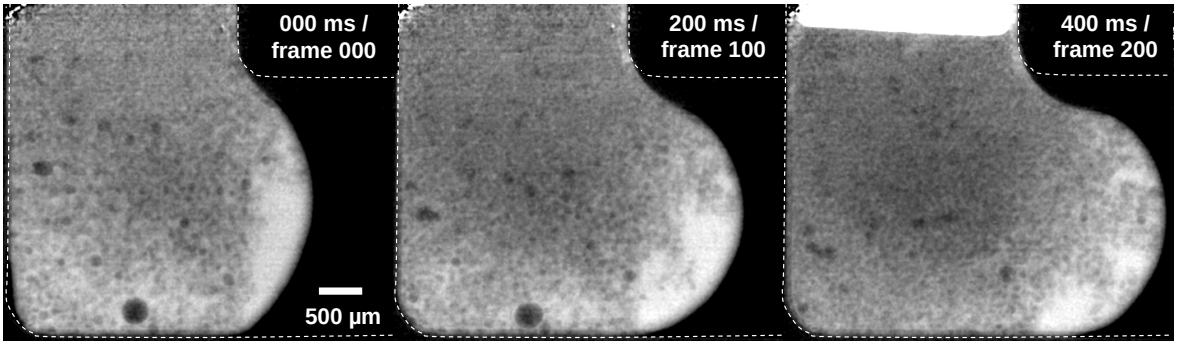

FIG. 3: Three selected radiographs showing the flow of semi-solid Al-Ge alloys through a channel with a right-angle turn (dashed line, 500 images/s acquisition speed). Each frame corresponds to 2 ms exposure time (acquired at the beamline ID15a of the ESRF, France). The gray values reflect a density / atomic number contrast: air (black), liquid melt (bright gray) and solid particles (dark gray).

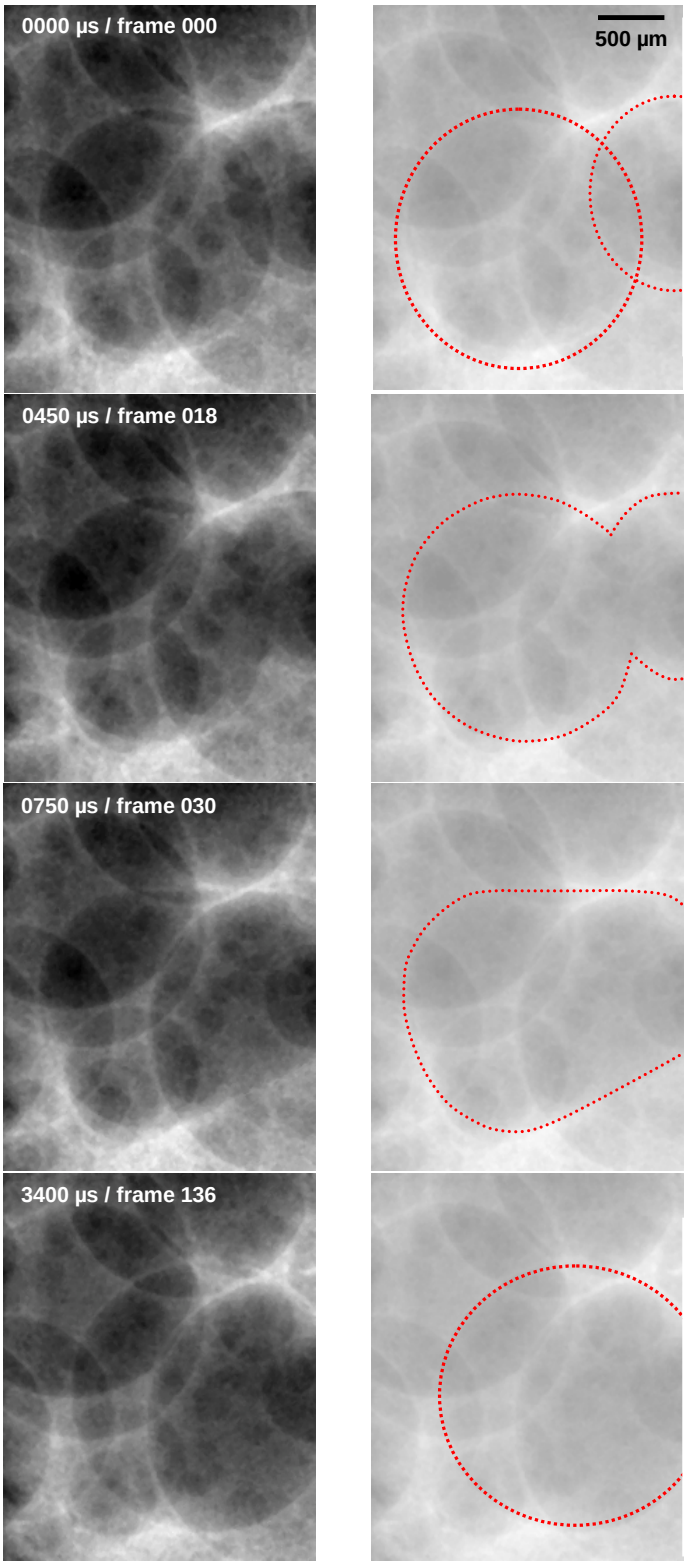

FIG. 4: Left column: image sequence taken out of a series of 184 000 (acquired at the beamline ID15a of the ESRF, France). Sequence shows a coalescence event inside a liquid metal foam (25 µs exposure time / 40 000 images/s, 20 µm effective pixel size, 192 × 192 pixel ROI); right column: sketch highlighting major features (see movie sequence deposited online [69]).

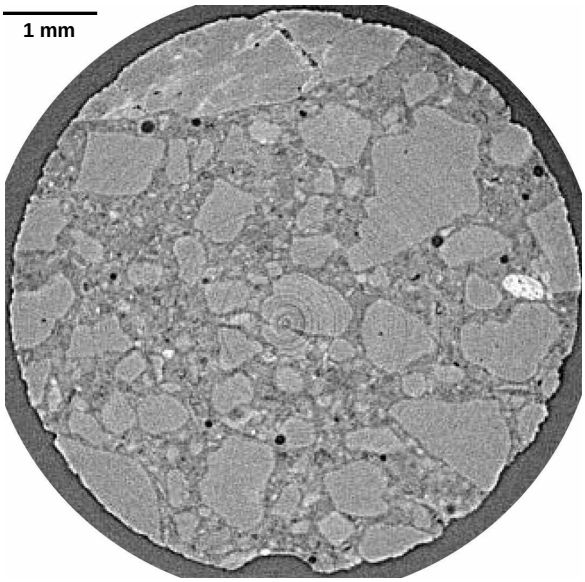

FIG. 5: Tomographic slice of a concrete specimen (kindly provided by Prof. Konietzky, TU Bergakademie Freiberg, Germany) imaged using polychromatic hard X-ray synchrotron radiation (acquired at the beamline ID15a of the ESRF, France). 1000 projection images were captured within 4 s, representing a 180° rotation of the specimen (diameter of the reconstructed slice is approximately 350 pixels). The CMOS-based camera Photron SA1 was used in combination with an indirect X-ray image detector. Several features are distinguishable within this multi-constituent specimen: pores as well as a highly absorbing impurities inside the sub-structured matrix.